



In Vitro Reconstitution of Functional Type III Protein Export and Insights into Flagellar Assembly

Hiroyuki Terashima,^{a*} Akihiro Kawamoto,^{b*} Chinatsu Tatsumi,^a Keiichi Namba,^{b,c} Tohru Minamino,^b Katsumi Imada^a

^aGraduate School of Science, Osaka University, Toyonaka, Osaka, Japan

^bGraduate School of Frontier Biosciences, Osaka University, Suita, Osaka, Japan

^cRIKEN Quantitative Biology Center, Suita, Osaka, Japan

ABSTRACT The type III secretion system (T3SS) forms the functional core of injectisomes, protein transporters that allow bacteria to deliver virulence factors into their hosts for infection, and flagella, which are critical for many pathogens to reach the site of infection. In spite of intensive genetic and biochemical studies, the T3SS protein export mechanism remains unclear due to the difficulty of accurate measurement of protein export *in vivo*. Here, we developed an *in vitro* flagellar T3S protein transport assay system using an inverted cytoplasmic membrane vesicle (IMV) for accurate and controlled measurements of flagellar protein export. We show that the flagellar T3SS in the IMV fully retains export activity. The flagellar hook was constructed inside the lumen of the IMV by adding purified component proteins externally to the IMV solution. We reproduced the hook length control and export specificity switch in the IMV consistent with that seen in the native cell. Previous *in vivo* analyses showed that flagellar protein export is driven by proton motive force (PMF) and facilitated by ATP hydrolysis by FliI, a T3SS-specific ATPase. Our *in vitro* assay recapitulated these previous *in vivo* observations but furthermore clearly demonstrated that even ATP hydrolysis by FliI alone can drive flagellar protein export. Moreover, this assay showed that addition of the FliH₂/FliI complex to the assay solution at a concentration similar to that in the cell dramatically enhanced protein export, confirming that the FliH₂/FliI complex in the cytoplasm is important for effective protein transport.

IMPORTANCE The type III secretion system (T3SS) is the functional core of the injectisome, a bacterial protein transporter used to deliver virulence proteins into host cells, and bacterial flagella, critical for many pathogens. The molecular mechanism of protein transport is still unclear due to difficulties in accurate measurements of protein transport under well-controlled conditions *in vivo*. We succeeded in developing an *in vitro* transport assay system of the flagellar T3SS using inverted membrane vesicles (IMVs). Flagellar hook formation was reproduced in the IMV, suggesting that the export apparatus in the IMV retains a protein transport activity similar to that in the cell. Using this system, we revealed that ATP hydrolysis by the T3SS ATPase can drive protein export without PMF.

KEYWORDS type III secretion system, bacterial flagellum, *in vitro* reconstitution, inverted membrane vesicle, protein transport

Type III secretion systems (T3SSs) are critical to the function of bacterial injectisomes and flagella. The injectisome is a bacterial protein transporter used to deliver virulence proteins into host cells for infection. The flagellum is a motile organelle critical for infection by many pathogens and is constructed by the T3SS built into the base of the flagellum.

The bacterial flagellum consists of a rotary motor spanning the cell envelope and a

Received 10 May 2018 Accepted 11 May 2018

Published 26 June 2018

Citation Terashima H, Kawamoto A, Tatsumi C, Namba K, Minamino T, Imada K. 2018. *In vitro* reconstitution of functional type III protein export and insights into flagellar assembly. mBio 9:e00988-18. <https://doi.org/10.1128/mBio.00988-18>.

Editor Richard Losick, Harvard University

Copyright © 2018 Terashima et al. This is an open-access article distributed under the terms of the [Creative Commons Attribution 4.0 International license](https://creativecommons.org/licenses/by/4.0/).

Address correspondence to Keiichi Namba, keiichi@fbs.osaka-u.ac.jp, or Katsumi Imada, kimada@chem.sci.osaka-u.ac.jp.

* Present address: Hiroyuki Terashima, Division of Biological Science, Graduate School of Science, Nagoya University, Nagoya, Japan; Akihiro Kawamoto, Institute for Protein Research, Osaka University, Suita, Osaka, Japan.

This article is a direct contribution from a Fellow of the American Academy of Microbiology. Solicited external reviewers: Judith Armitage, University of Oxford; Morgan Beeby, Imperial College London.

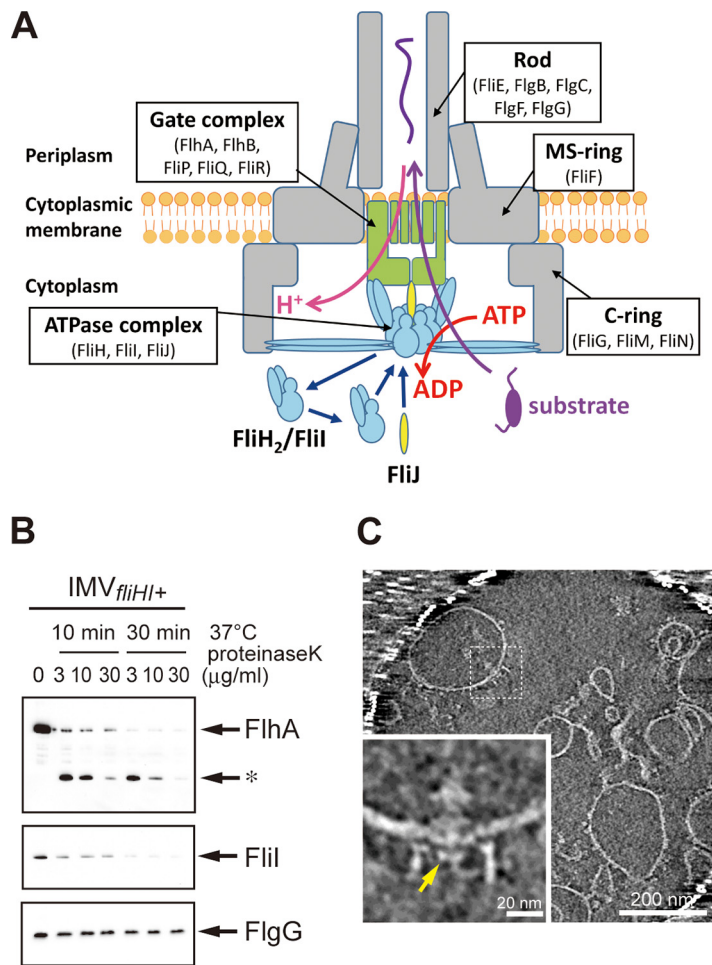


FIG 1 Verification of inverted membrane vesicle (IMV) formation. (A) Schematic drawing of the flagellar protein export apparatus in the basal body. The transmembrane gate components are colored in green. FliH and FliI are shown in cyan, and FliJ is shown in yellow. Substrate proteins are shown in purple. The FliH₂/FliI complex is attached to the gate complex and the C-ring through FliH. (B) Digestion of flagellar proteins in the IMV with proteinase K. The IMV solution was mixed with proteinase K (3, 10, or 30 μg/ml) and incubated at 37°C. The reactants were sampled after 0, 10, and 30 min of incubation and were then analyzed by immunoblotting. FlhA (top panel) and FliI (middle panel) were degraded by proteinase K, but FlgG (bottom panel) was retained, indicating that the membrane is surely inverted. The asterisk indicates a partially degraded intermediate of FlhA. (C) Electron cryotomographic image of the IMVs. The lower left panel is a magnified image of the basal body in the IMV. The disk-like density is indicated by a yellow arrow.

filamentous axial structure extending out from the cell surface. The axial structure is a tubular, helical protein assembly composed of more than 20,000 protein subunits of about 10 different proteins. These axial proteins and their assembly scaffold proteins, such as FlgJ, FlgD, and FliD, are translocated via the flagellar T3SS, the flagellar protein export apparatus, across the cytoplasmic membrane into the central channel of the growing flagellum. The flagellar protein export apparatus consists of the transmembrane gate complex formed by FlhA, FlhB, FliP, FliQ, and FliR and the cytoplasmic ATPase complex composed of FliH, FliI, and FliJ (1–3) (Fig. 1A). It was thought that FliO is also one of the transmembrane gate proteins, but a recent study revealed that it only facilitates the assembly of the export gate complex (4). Except for FliO, these proteins share sequence homologies with those of injectisome T3SSs in pathogenic bacteria (5). The gate complex is located in the central pore of the basal body MS-ring, and the ATPase complex is bound just below the gate complex in the cytoplasm through the interactions with the gate and the basal body C-ring (6). FliI is a Walker-type ATPase (7) and is homologous to the α and β subunits of F₁-ATPase in structure (8). FliI and FliJ

together form the FliI₆/FliJ complex that is similar to the F₁-α₃β₃γ complex, suggesting that the FliI₆/FliJ complex hydrolyzes ATP in a way similar to F₁-ATPase (9). FliH forms a homodimer similar to the peripheral stalk of V-ATPase (10) and binds to the N-terminal domain of FliI in a way similar to F- and V-type ATPases (11, 12). While FliH is indispensable for efficient formation of the FliI₆/FliJ complex at the flagellar base (13), FliH also regulates the ATPase activity of FliI negatively by forming the FliH₂/FliI complex and suppresses the hexamerization of FliI in solution (11, 12). The FliH₂/FliI complex binds to late export substrates in complex with their cognate chaperones (14–16) and ensures the interaction between the chaperone-substrate complex and FlhA (17), but the details are unclear.

Flagellar protein transport is primarily driven by proton motive force (PMF) (18, 19). FlhA has an ion channel activity, and the FlhA-FliJ interaction enables effective utilization of PMF for protein export (20). Since infrequent ATP hydrolysis by FliI ATPase with the E211D substitution is sufficient for processive protein export for flagellar formation, the energy of ATP hydrolysis by FliI is thought to be required primarily for gate activation (18, 19, 21, 22). A study on the virulence T3SS ATPase InvC has suggested that the energy of ATP hydrolysis is used to unfold substrate proteins for export (23). However, it has been shown that the ATPase activity of InvC is not essential for protein unfolding (24). Therefore, it is still controversial how these two types of energy are used in the protein export mechanism.

Despite many genetic and biochemical studies on the T3SSs, the molecular mechanism of protein transport is still obscure due to difficulties in accurate measurements of protein transport under precise control of measurement conditions *in vivo*. Therefore, an *in vitro* transport assay system with easy control of measurement conditions is needed for further in-depth mechanistic understanding of protein transport. The inverted membrane vesicle (IMV)-based assay has been used for studying protein translocation across the cell membrane (25), such as the Sec machinery (26) and the twin arginine translocation (TAT) machinery (27), but has never been applied to supramolecular complexes such as the T3SS. We have developed an IMV-based flagellar protein transport assay system that enables accurate measurements of protein transport under well-controlled conditions. The export apparatus in the IMV preserves the protein transport activity. The formation of the flagellar hook about 55 nm in length was reproduced in the IMV, and the export apparatus in IMV retains the protein transport function at a similar level as that in the cell. Surprisingly, even ATP hydrolysis by FliI alone was able to drive flagellar protein export without PMF. We discuss the molecular mechanism of protein transport on the basis of this novel protein transport assay.

RESULTS

Preparation of inverted membrane vesicles. The IMVs were prepared from a *Salmonella* Δ*fliT* Δ*flgD* Δ*flhB* mutant strain expressing FlhB(N269A) and FlhD/FlhC. We used a *fliT* null and FlhD/FlhC-overexpressed mutant because deletion of the *fliT* gene and overexpression of FlhD/FlhC increase the number of the flagellar basal bodies per cell (28). We also introduced a *flgD* null mutation allele because we used purified FlgD to evaluate the protein transport activity of IMV. FlgD has most frequently been used for our *in vivo* export analysis of the flagellar T3SS because of the sensitivity and quality of our polyclonal anti-FlgD antibody for measuring the amount of FlgD. FlgD is a scaffolding protein required for the flagellar hook formation. FlgD forms a cap complex at the distal end of the growing hook, and the hook protein FlgE is incorporated into the growing hook just beneath the cap complex (29, 30). Therefore, the hook is not formed without FlgD. FlgD and FlgE are rod-hook-type proteins and need no specific chaperones for export. The flagellar export apparatus switches export specificity from rod-hook-type proteins to filament-type proteins upon completion of hook assembly (2); hence, we introduced the FlhB(N269A) mutation to lock the export apparatus in the rod-hook-type protein export mode (31). FlhB undergoes autocleavage between N269 and P270, and the autocleavage is a critical event for the export specificity switch.

Therefore, the FlhB(N269A) mutation completely inhibits the cleavage and locks the export apparatus in the rod-hook-type protein export mode.

The cells were converted to spheroplasts by treatment with EDTA and lysozyme to remove the outer membrane and the peptidoglycan layer, respectively, and were then disrupted by a high-pressure homogenizer to produce inside-out vesicles. The vesicles were purified by sucrose density gradient centrifugation. The vesicles contained FlhA and FlhB (membrane components); FliH, FliI, and FliJ (soluble components); FliF (MS-ring component); and FliG, FliM, and FliN (C-ring components) as judged by immunoblotting (see Fig. S1A in the supplemental material). To verify the membrane orientation, the vesicles were incubated with proteinase K, followed by immunoblotting with polyclonal anti-FlhA, anti-FliI, and anti-FlgG antibodies. FlhA and FliI were degraded (Fig. 1B, top and middle panels), indicating that they are present outside the membrane vesicles. In contrast, FlgG (a rod protein) was resistant to proteolysis (Fig. 1B, bottom panel), indicating that it is inside the vesicles. FlhA and FliI are located on the cytoplasmic side of the export apparatus, whereas FlgG is located in the periplasm. Thus, we concluded that the orientation of the membrane vesicles is inside-out. The formation of the IMV was further confirmed by electron cryotomography (ECT). We observed the flagellar basal body embedded in the membrane with the C-ring exposed on the outside of the vesicle (Fig. 1C). A disk-like density identified as the cytoplasmic domain of FlhA in the previous ECT analysis of *Salmonella* and *Campylobacter jejuni* (6, 32) was observed within the C-ring (Fig. 1C), suggesting that the basal body in the IMV retains the membrane components of the export apparatus. No clear spherical density corresponding to the ATPase complex (33) was observed below the disk-like density. However, we often found some density probably corresponding to a partially disrupted ATPase complex during IMV preparation.

IMV preserves the protein transport activity. The protein transport activity of the export apparatus in the IMV was examined by measuring the amount of FlgD transported into the vesicles. After incubation of the IMVs with purified FlgD in a buffer solution containing 20 mM Tris-HCl, pH 7.5, and 125 mM KCl, followed by proteinase K treatment to digest the external proteins, the transported proteins were monitored by immunoblotting with polyclonal anti-FlgD antibody. FliJ was added in the reaction mixture in all experiments except for the experiments below, because it is essential to efficiently couple PMF with protein export (21). FlgD was transported into the IMVs in the presence of ATP, Mg^{2+} , and FliJ in the external solution (Fig. 2A). No FlgD transport was observed for the IMVs prepared from the *flhB* null mutant cells (IMV $_{\Delta flhB}$), which do not have protein export activity *in vivo* (18) (Fig. S2A). In agreement with previous *in vivo* experiments (18, 19), protein transport was suppressed by a proton-specific ionophore, carbonyl cyanide *m*-chlorophenylhydrazine (CCCP) (Fig. 2A and B). These results indicate that the export apparatus in the IMVs preserves the export activity.

PMF across the cytoplasmic membrane is maintained by proton pumping by the reverse reaction of endogenous F_0F_1 -ATP synthase in our assay system, although the initial PMF was produced by using IMVs filled with a solution containing 20 mM morpholinoethanesulfonic acid (MES)-NaOH, pH 6.0, and 300 mM NaCl. Mg^{2+} and ATP were both indispensable for FlgD transport in the IMV assay, and Mg^{2+} could not be replaced by Ca^{2+} (Fig. S2B). No FlgD was transported into the IMV when ADP or AMPPNP was used instead of ATP (Fig. S2B), and the amount of transported FlgD depended on the ATP concentration (Fig. S2C). This Mg^{2+} -ATP dependence was also detected for the IMVs prepared from the *fliH-fliI* null mutant cells (IMV $_{\Delta fliH/\Delta fliI/\Delta pH/pNa}$) (Fig. 2C) or in the IMVs filled with the same solution as the external buffer (IMV $_{fliH/+/-\Delta pH/pNa}$) to deplete the initial pH and ion concentration gradients (Fig. 2D). Moreover, the FlgD transport was suppressed by the addition of CCCP for IMV $_{\Delta fliH/\Delta fliI/\Delta pH/pNa}$ and IMV $_{fliH/+/-\Delta pH/pNa}$ (Fig. 2C and D). These results suggest that endogenous ATPases, such as F_0F_1 -ATP synthase, generate PMF using the energy of ATP hydrolysis. Addition of F_0F_1 -ATP synthase inhibitors strongly suppressed FlgD transport, supporting the contribution of F_0F_1 -ATP synthase to the PMF generation (Fig. 2E). To confirm the contribution of F_0F_1 -ATP

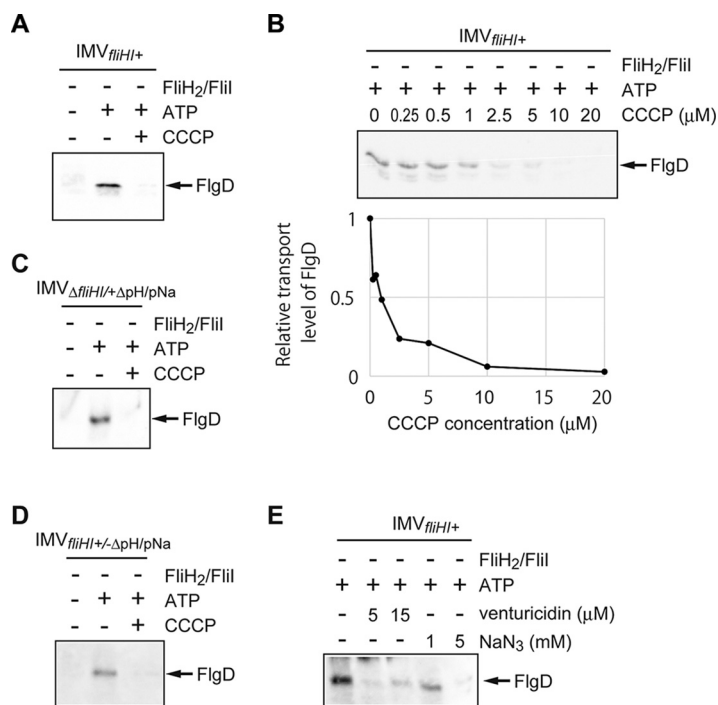


FIG 2 Evidence for inverted membrane vesicles (IMVs) preserving the flagellar protein export activity. *In vitro* protein transport assays were conducted with IMV_{fliH+} (normal IMVs; *fliH*⁺/⁺ΔpH/pNa) (A, B, and E), IMV_{ΔfliH/+ΔpH/pNa} (Δ*fliH*/⁺ΔpH/pNa) (C), or IMV_{fliH+/-ΔpH/pNa} (*fliH*⁺/⁻ΔpH/pNa) (D). FlgD transported into the IMV was analyzed by immunoblotting with polyclonal anti-FlgD antibody. (A) The FlgD transport required ATP and was inhibited by CCCP. The transport assay was conducted with (+) or without (-) 5 mM ATP or 10 μM CCCP. The concentrations of FlgD and FliJ in the reaction mixture were 4 μM and 0.25 μM, respectively. (B) The FlgD transport was suppressed with the increase of CCCP concentration (upper panel). The transport levels of FlgD relative to that without CCCP are shown (lower panel). The concentrations of FlgD, FliJ, and ATP in the reaction mixture were 4 μM, 0.25 μM, and 5 mM, respectively. (C to E) Effect of PMF generated by endogenous F_oF₁-ATP synthase on the protein transport into the IMV. (C and D) FlgD transport assay for IMV_{ΔfliH/+ΔpH/pNa} (C) and IMV_{fliH+/-ΔpH/pNa} (D). The transport assay was conducted with (+) or without (-) ATP (5 mM) and CCCP (10 μM). The concentrations of FlgD and FliJ in the reaction mixture were 4 μM and 0.25 μM, respectively. The FlgD transport required ATP and was inhibited by addition of CCCP. (E) The FlgD transport was suppressed by the F_oF₁-ATP synthase inhibitors. The transport assay was carried out with venturicidin (5 or 15 μM) or NaN₃ (1 or 5 mM). The leftmost lane is a control. The concentrations of FlgD, FliJ, and ATP in the reaction mixture were 4 μM, 0.25 μM, and 5 mM, respectively.

synthase, we altered the F_oF₁-ATP synthase locus (subunits α, β, γ, δ, ε, A, B, C, and I) of *Salmonella* strain STH002 (Δ*flhB* Δ*flgD* Δ*fliT* Δ*fliH*) to tetracycline resistance genes (*tetRA*) and prepared the IMV (IMV_{ΔF_oF₁-ΔfliH}). Deletion of F_oF₁-ATP synthase considerably decreased FlgD transport (see Fig. 5A), suggesting that the protein transport by the IMV is mainly driven by PMF generated by the reverse reaction of F_oF₁-ATP synthase.

The FliH₂/FliI complex in solution is essential for efficient protein transport.

While the FliI₆ ring complex associates with the basal body through the interactions of FliH with FlhA and FliN, FliI shows turnovers between the basal body and the cytoplasmic pool in an ATP-independent manner (34), raising the possibility that the FliH₂/FliI complex present in the cytoplasm is needed for the protein export. To examine this hypothesis, we added the FliH₂/FliI complex with FliJ to the external solution and found that the FlgD transport into the IMVs was dramatically enhanced (Fig. 3A, upper panel). The transport enhancement was also observed for the IMVs prepared from the *fliH*-*fliI* null mutant cells (IMV_{ΔfliH}) (Fig. 3A, lower panel). These results show that the FliH₂/FliI complex externally added in solution can assemble onto the export gate complex to form a functional export apparatus. Individual addition of either FliJ or the FliH₂/FliI complex promoted FlgD transport only slightly (Fig. 3A), which is consistent with previous observations that *fliH*-*fliI* double null mutant and *fliJ* null

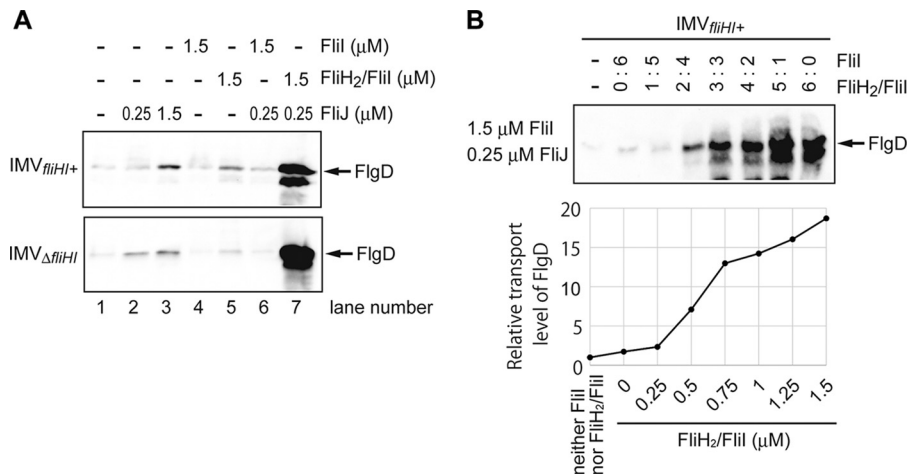


FIG 3 Additive effect of the soluble components of the flagellar protein export apparatus on FlgD transport. FlgD transported into the IMV was detected by immunoblotting. (A) Transport assay with or without soluble component proteins using the normal IMV (*fliH*⁺) (upper panel) or the *FliH*-deficient IMV (Δ *fliH*) (lower panel). The concentrations of FlgD and ATP in the reaction mixture were 4 μ M and 5 mM, respectively. The FlgD transport was markedly increased by addition of both FliJ and the *FliH*₂/*FliI* complex. Individual addition of FliJ or the *FliH*₂/*FliI* complex also facilitated the FlgD secretion to some extent. (B) The transport assay in the presence of *FliI* and the *FliH*₂/*FliI* complex at various ratios (upper panel). The transport levels of FlgD relative to that without *FliI* or the *FliH*₂/*FliI* complex are shown (lower panel). The FlgD transport was enhanced by the *FliH*₂/*FliI* complex but not by *FliI*. The total concentration of *FliI* was kept at 1.5 μ M. The FliJ concentration was adjusted to 1/6 of the *FliI* concentration. The concentration of ATP in the reaction mixture was 5 mM. The leftmost lane is the negative control (*FliI* and the *FliH*₂/*FliI* complex were not added).

mutant strains both show a weakly motile phenotype (18, 19). In contrast, addition of *FliI* alone did not affect FlgD transport at all (Fig. 3A). These findings indicate that the *FliH*₂/*FliI* complex and FliJ cooperatively act on the protein export mechanism. It is possible that *FliH*/*FliI* could fall off during IMV preparation because the *FliI* density is lost in cryotomograms of lysed cells in the previous studies (33). Then, we preincubated IMVs with the *FliH*₂/*FliI* complex and conducted the transport assay. Preincubation alone showed only a slight enhancement of the FlgD transport (Fig. S3). The effect of the *FliH*₂/*FliI* complex in solution containing purified FliJ was further examined by changing the concentration of the *FliH*₂/*FliI* complex. The transport assay was performed in solution containing *FliI* and the *FliH*₂/*FliI* complex at various molar ratios with the total amount of *FliI* kept constant. The concentration of FliJ was adjusted to 1/6 of the total *FliI* concentration because a small amount of FliJ facilitates the ATPase complex formation but an excess amount of FliJ inhibits *FliI* hexamer formation (9). The level of FlgD transport was increased considerably with an increase in the amount of the *FliH*₂/*FliI* complex (Fig. 3B). Therefore, we conclude that the *FliH*₂/*FliI* complex in solution is essential for efficient protein export.

FlgD facilitates FlgE export. We next examined the transport of another substrate, FlgE, to investigate hook formation inside the vesicle. We added purified FlgE with or without FlgD in the external solution and performed the *in vitro* protein transport assay. In the presence of FlgD, the transported FlgE monomers assembled into the hook structure on the basal body, resembling those seen in unperturbed cells (Fig. 4A and Fig. S4), indicating that hundreds of FlgE molecules were processively transported into the IMV via a single export apparatus to form a bona fide hook. Interestingly, the amount of transported FlgE was increased by about two times in the presence of FlgD, indicating that FlgD facilitates FlgE export into the IMVs in addition to chaperoning assembly (Fig. 4B).

***In vitro* hook length control.** The length of the wild-type hook is regulated at about 55 (\pm 6) nm by FliK, a molecular ruler that measures the hook length. After reaching its mature length, FliK interacts with FlhB to switch the export specificity from rod-hook-

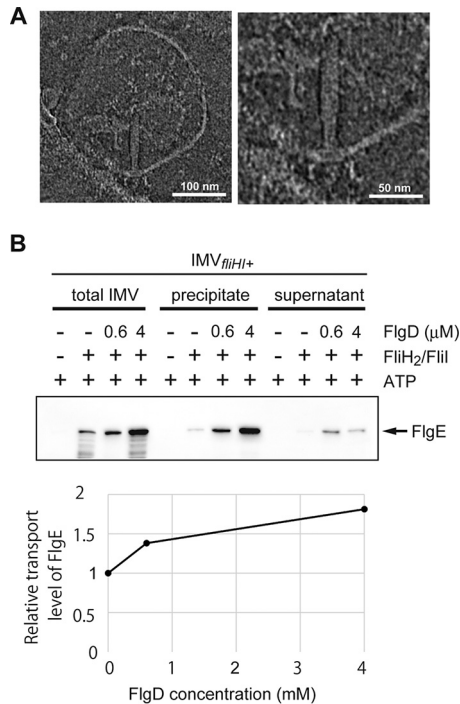


FIG 4 The hook formation inside the IMV. (A) Electron cryotomographic images of the hook formed on the basal body inside the IMV. A representative image is shown in the left panel, and its magnified image is shown in the right panel. The transport assay was conducted with FlgD (4 μM), FlgE (4 μM), the FliH₂/FliI complex (1.5 μM), and FliJ (0.25 μM) using the normal IMV (*fliH⁺*). The concentration of ATP in the reaction mixture was 5 mM. (B) FlgE transport is facilitated by FlgD (upper panel). The transport levels of FlgE relative to that in the absence of FlgD are shown (lower panel). The transport assay was conducted with (+) or without (–) FlgD (0.6 μM or 4 μM) and the FliH₂/FliI complex (1.5 μM). The concentrations of FlgE, FliJ, and ATP in the reaction mixture were 4 μM, 0.25 μM, and 5 mM, respectively. The concentration of K⁺ (KCl and ATP/2K-KOH) in the reaction mixture was adjusted to 133 mM. FlgE transported into the IMV was analyzed by immunoblotting. To analyze the hook formation, we collected the basal body. Part of the reactant was centrifuged (150,000 × *g* for 30 min) after treatment with proteinase K and Triton X-100. The supernatant and the precipitate were analyzed by immunoblotting. In the presence of FlgD at a sufficiently high concentration, most of the FlgE transported into the IMV was detected in the precipitate, indicating that the transported FlgE formed the hook structure.

type to filament-type proteins (2). We tried to reproduce the hook length control and the export specificity switch in the IMV prepared from a *Salmonella* Δ*fliT* Δ*flgD* Δ*flhB* mutant strain expressing wild-type FlhB and FlhD/FlhC by adding purified FliK at various concentrations into the reaction mixture. After a 1-h reaction, we purified the hook-basal bodies from the IMV and measured the hook length by negative-staining electron microscopy (EM). Polyhooks with various lengths were produced without FliK, but with the increase of FliK concentration, the average length became shorter and the length distribution became narrower (Fig. S5). In the presence of 4 μM FliK, the average length was successfully controlled at about 55 (±22) nm, suggesting that no soluble component other than FliK is necessary for the hook length control and substrate specificity switch. The standard deviation (SD) of the hook length was larger than that of the wild-type hook but was similar to that for the cells overproducing FlgE (35). The FlgE concentration used for this assay (4 μM) corresponds to about 4,000 molecules/cell, and this is presumably much higher than the cellular level. The large SD of the hook length may be due to this high concentration of FlgE.

ATP hydrolysis by FliI can drive the protein export without PMF. As described above, the protein transport by the IMV is mainly driven by PMF generated by the reverse reaction of F_oF₁-ATP synthase. However, FlgD transport was still retained to some extent without F_oF₁-ATP synthase, even in the absence of the pH and ion concentration gradients, when the FliH₂/FliI complex, FliJ, and Mg²⁺-ATP were present in the external solution (Fig. 5A), suggesting that protein export can be driven solely by

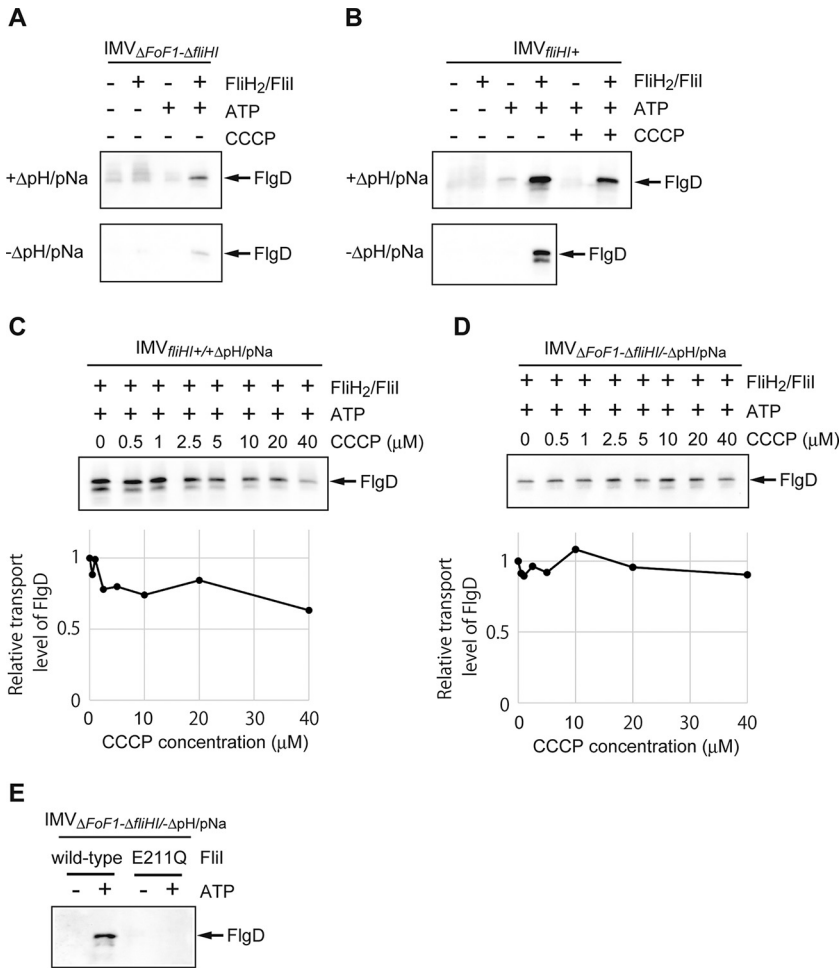


FIG 5 Protein transport driven by ATP hydrolysis. FlgD transported into the IMV was analyzed by immunoblotting. (A) ATP drives the protein transport without PMF. FlgD transport by the IMV_{ΔFoF1-ΔfliHl} (ΔFoF1-ΔfliHl/+ΔpH/pNa) (upper panel) and IMV_{ΔFoF1-ΔfliHl-ΔpH/pNa} (ΔFoF1-ΔfliHl/-ΔpH/pNa) (lower panel). The transport assay was conducted with (+) or without (-) the FliH₂/FliI complex (1.5 μM) and ATP (5 mM). The concentrations of FlgD and FliJ in the reaction mixture were 4 μM and 0.25 μM, respectively. The faint smear bands of the first, second, and third lanes in the upper panel are nonspecific signals. (B) FlgD transport by the normal IMV (fliHl⁺/+ΔpH/pNa) (upper panel) and IMV_{fliHl+/+ΔpH/pNa} (fliHl⁺/-ΔpH/pNa) (lower panel). The transport assay was conducted with (+) or without (-) the FliH₂/FliI complex (1.5 μM), ATP (5 mM), and CCCP (10 μM). The concentrations of FlgD and FliJ in the reaction mixture were 4 μM and 0.25 μM, respectively. The FlgD transport of the IMV_{fliHl+} was decreased in the presence of CCCP but still remained in the presence of the FliH₂/FliI complex. The faint smear bands of the first and second lanes in the upper panel are nonspecific signals. (C) The FlgD transport of the normal IMV (IMV_{fliHl+/+ΔpH/pNa}) in the presence of the FliH₂/FliI complex and FliJ was suppressed with the increase in the CCCP concentration (upper panel). The transport levels of FlgD relative to that without CCCP are shown (lower panel). The concentrations of FlgD, the FliH₂/FliI complex, FliJ, and ATP in the reaction mixture were 4 μM, 1.5 μM, 0.25 μM, and 5 mM, respectively. (D) Effect of CCCP on the ATP-driven protein transport (upper panel). The transport levels of FlgD relative to that without CCCP are shown (lower panel). The FlgD transport assay was performed using IMV_{ΔFoF1-ΔfliHl-ΔpH/pNa}. The concentrations of FlgD, the FliH₂/FliI complex, FliJ, and ATP in the reaction mixture were 4 μM, 1.5 μM, 0.25 μM, and 5 mM, respectively. (E) ATP hydrolysis activity of FliI and the protein transport activity in the absence of PMF. The FlgD transport assay was carried out with the FliH₂/FliI complex (1.5 μM) or the FliH₂/FliI(E211Q) complex (1.5 μM) with (+) or without (-) ATP (5 mM) using IMV_{ΔFoF1-ΔfliHl-ΔpH/pNa}. The concentrations of FlgD and FliJ were 4 μM and 0.25 μM, respectively.

ATP hydrolysis by the FliI ATPase. To confirm protein transport without PMF, we added CCCP in the reaction mixture containing FliJ, the FliH₂/FliI complex, and Mg²⁺-ATP. The FlgD export activity of the IMV_{fliHl+} was reduced in the presence of CCCP but was still significantly retained (Fig. 5B and C). To verify protein transport without PMF, we performed a transport assay using IMV_{ΔFoF1-ΔfliHl} without pH and ion concentration gradients (Fig. 5A, lower panel, and D). The FlgD export activity of IMV_{ΔFoF1-ΔfliHl} was not

affected at all by CCCP up to 40 μM in the presence of FliJ, the FliH₂/FliI complex, and Mg²⁺-ATP (Fig. 5D). We further tested hook formation without PMF. IMV _{$\Delta\text{Fof1-}\Delta\text{fliH}$} mixed with FlgD, FlgE, FliJ, and the FliH₂/FliI complex was incubated with or without Mg²⁺-ATP for 1 h. Then, basal bodies were purified from the IMV and observed by negative-staining EM. Polyhooks were formed in the presence of 5 mM ATP and even with 10 μM CCCP but not without ATP (Fig. 5G). These results indicate that processive transport of FlgE occurs even in the absence of PMF when FliJ, the FliH₂/FliI complex, and Mg²⁺-ATP are present. To examine if ATP hydrolysis by FliI is responsible for the protein export without PMF, we added the FliH₂/FliI(E211Q) complex to the reaction mixture instead of the FliH₂/FliI complex. FliI(E211Q) can bind Mg²⁺-ATP to form a hexameric ring and associate with the export gate but has no ATP hydrolyzing activity (36). Unlike with wild-type FliI, FlgD was not transported into the IMVs (Fig. 5E). Therefore, we conclude that flagellar protein export can be driven by ATP hydrolysis by FliI in the absence of bulk PMF.

DISCUSSION

The flagellar export apparatus transports 20,000 to 30,000 protein subunits of 14 different proteins. Therefore, the coordination of protein export is important to construct the flagellum. The substrate specificity of the export apparatus is switched from rod-hook-type proteins to filament-type proteins after completion of the hook, and the substrate specificity switch is coupled to the gene expression of each type of protein (2). The export of filament-type proteins is coordinated by the flagellar type III export chaperones. These chaperones bind to their specific cognate substrates (37–40). The binding affinity of the chaperone/substrate complexes for FlhA, an export gate protein, is thought to regulate the secretion order of the filament-type proteins (41, 42). Rod-hook-type substrates bind to a well-conserved hydrophobic pocket of the C-terminal cytoplasmic domain of FlhB (43). Recent genetic analyses have suggested that FliH, FliI, FlhA, and FlhB coordinate hook-type protein export with hook assembly to regulate the hook length at 55 nm in *Salmonella* (44). However, the coordination of rod-hook-type protein export was not well known, and no such export chaperones were found for rod-hook-type proteins. We observed that export of FlgE is facilitated by FlgD. FlgD and FlgE are both rod-hook-type export substrates and are supposed to compete for their transport. Thus, FlgE transport should be decreased by an addition of FlgD as seen *in vivo* (45). However, to the contrary, FlgE transport was increased by about two times in the presence of an equal amount of FlgD. This result suggests the presence of a cooperative mechanism between rod-hook-type proteins for efficient and ordered protein export. The enhancement of FlgE export by FlgD is reasonable because the FlgD cap formation is needed prior to the hook formation (29).

The FlgD transport was 20 times enhanced in the presence of 1.5 μM FliH₂/FliI in the reaction mixture. The number of FliI molecules in a cell was estimated to be 1,500 (46). If we assume that the bacterial cell is a rod-shaped cylinder with a length of 1.5 μm and a diameter of 1 μm capped by hemispherical ends with a diameter of 1 μm , the bacterial cell volume is 1.7 fl, and the concentration of FliI in a cell is estimated to be 1.5 μM . This value is comparable to our experimental condition, implying that a certain amount of the FliH₂/FliI complex in the cytoplasm is needed for efficient protein export. Then, what is the role of the FliH₂/FliI complex in solution? *In situ* electron cryotomography revealed that the FliI hexamer complex is associated with the basal-body C-ring through FliH (6, 10, 34), but the FliI hexamer complex has never been observed in the purified basal body *in vitro*, or lysed cells for electron cryotomography (33), indicating that an interaction between the FliH/FliI complex and the basal body is not so strong. Moreover, turnover of FliI between the basal body and the cytoplasmic pool has been demonstrated by fluorescence recovery after photobleaching (FRAP) experiments (34). Thus, a certain amount of the FliH₂/FliI complex in the cytoplasm may be required for stable association and turnover of the FliI hexamer to the basal body.

Previous *in vivo* studies have revealed that flagellar type III protein export is driven by proton motive force (PMF) and facilitated by ATP hydrolysis by FliI ATPase (18, 19).

In agreement with the *in vivo* experiments, protein transport of IMV_{ΔfliH} was observed and inhibited by CCCP. Because the diameter of the central channel of the rod and hook for the substrate passage is only 1.3 nm (47), the substrate proteins must be unfolded during their translocation through the channel. We used purified FlgD and FlgE for a transport assay, and IMV_{ΔfliH} transported these substrate without any help from other proteins except for FliJ (Fig. 2C and 3A). Size exclusion chromatography, which is the final purification step, showed a symmetrical elution peak around the expected molecular weight for each protein. The purified FlgD has been crystallized, and the structure will be published elsewhere. These results indicate that the purified FlgD and FlgE are both well folded in solution. Therefore, our results suggest that the transmembrane gate complex itself has the unfolding activity of substrate proteins. On the other hand, our IMV assay indicates that ATP hydrolysis by FliI can drive the protein export without bulk PMF. Protein transport without PMF was not detected in the previous *in vivo* experiment. In our *in vitro* experiments, the concentration of the substrate was higher than in the *in vivo* experiments and was kept constant. Moreover, the concentrations of the FliH₂/FliI complex and FliJ were also kept constant. These conditions may enable us to detect the protein transport without PMF. It is still unclear how the cytoplasmic ATPase complex unfolds the export substrate and opens the transmembrane gate. Since the entire structure of the ATPase complex is very similar to that of F_oF₁-ATP synthase (8–10), and ATP hydrolysis is closely linked to efficient proton translocation (48), one possibility is that local PMF is generated by the ATPase complex, and the transmembrane gate complex exports the substrates using this local PMF. *In vivo* local pH measurement using pHluorin(M153R) revealed that the ATPase activity of FliI reduced local pH near the export apparatus (48). Moreover, ΔpH is not required for protein export in the presence of FliH and FliI (21). These previous results support this idea, but further investigation is needed to understand the role of ATP hydrolysis by FliI. The Sec protein translocation system requires both PMF and ATP (26), while the TAT system needs only PMF (27). Our study revealed that, unlike these two systems, both PMF and ATP hydrolysis can drive the flagellar type III protein export, although they are both needed for the maximum secretion activity. This energetic redundancy may contribute to the robustness of the flagellar protein export apparatus that is essential for bacterial motility.

Development of an *in vitro* transport assay system with easy control of measurement conditions is important for mechanistic understanding of protein transport. The IMV-based assay has been used for studying various transporters and greatly contributed to the elucidation of the molecular mechanism of substrate transport across the cell membrane (25–27). However, the IMV-based technique has been used only for the transporter consisting of a few to a dozen protein subunits. We applied this technique to the flagellar export machinery, which is composed of more than 250 protein subunits of 12 different types of proteins (FliF, FliG, FliH, FliI, FliJ, FliM, FliN, FliP, FliQ, FliR, FliA, and FliB), including the housing of the export apparatus. The export apparatus translocated purified substrate proteins from the external solution into the lumen of the IMV. In addition, the hook length control and the export specificity switching were reproduced in the IMV. These results suggest that the export apparatus in the IMV retains its native function as in the cell. The IMV-based *in vitro* assay described here may also be applied to other large membrane complex systems that are difficult to purify or isolate from the cell membrane in the fully functional form. The *in vitro* system of course cannot fully reproduce the cellular condition, including molecular crowding and complex interactions between various molecules, and therefore the measurement results with the IMV-based system do not directly reflect the cellular events. However, even with such limitations, this IMV-based method will be a useful tool for studying the functional mechanisms and structures of such large complex systems.

MATERIALS AND METHODS

Bacterial strains and plasmids. Bacterial strains and plasmids are listed in Table S1 in the supplemental material. *Salmonella* and *Escherichia coli* were cultured in LB broth (1% [wt/vol] Bacto tryptone,

0.5% [wt/vol] yeast extract, 0.5% [wt/vol] NaCl). Chloramphenicol was added to a final concentration of 30 $\mu\text{g/ml}$. Ampicillin was added to a final concentration of 50 $\mu\text{g/ml}$.

Preparation of the cells. The cells used for IMV preparation were constructed from a *Salmonella* mutant strain with deletion of *flhB*, *flgD*, and *fliT*. The cells were transformed with a pBAD33-based plasmid harboring *flhB*(N269A) and *flhDC*, into the mutant cell. To increase the number of flagellar basal bodies, we deleted *fliT*, the negative regulator of the flagellar class 2 gene, and expressed *flhDC*, the master regulator of the flagellar genes. The *flgD* gene was also deleted, because we selected FlgD as a standard substrate for the transport assay. To prevent the substrate specificity switching from rod-hook-type to filament-type proteins, *flhB* was deleted and the *flhB* N269A mutant gene was introduced. The IMVs used for the hook length control and export switch experiment were prepared from the cells harboring wild-type *flhB* instead of *flhB* N269A.

Preparation of inverted membrane vesicles. Overnight cell culture was inoculated into 1 liter of fresh LB broth in a 5-liter flask with 1/100 dilution and cultured at 30°C for 1 h. L-Arabinose was added to the final concentration of 0.02% (wt/vol), and the culture was continued at 18°C for 12 to 16 h (until optical density at 600 nm [OD₆₀₀] reached around 1.5). The cells were collected, suspended into 75 ml of sucrose solution (10 mM Tris-HCl, pH 8.0, 0.75 M sucrose) and stirred with 22.5 mg of lysozyme on ice. Then, 150 ml of 1.5 mM EDTA was poured onto the suspension on ice, and stirring was continued for 1 h at 4°C. The cells were collected at 5,000 $\times g$ and suspended into 25 ml solution A (20 mM MES-NaOH, pH 6.0, 300 mM NaCl) or solution B (20 mM Tris-HCl, pH 7.5, 125 mM KCl) with 1 tablet of protease inhibitor Complete EDTA-free (Roche). The suspension was passed through a high-pressure cell homogenizer (Stansted) at 90 MPa to produce inverted-membrane vesicles. After removal of debris by centrifugation at 20,000 $\times g$ for 10 min, IMVs were precipitated by ultracentrifugation at 100,000 $\times g$ for 1 h. IMVs were suspended into 1 ml of solution A or B and purified by sucrose density gradient centrifugation (60% [wt/wt] 5 ml, 50% [wt/wt] 9 ml, 45% [wt/wt] 9 ml, 40% [wt/wt] 6 ml stepwise gradient in a Beckman ultraclear tube) at 60,000 $\times g$ (SW32 Ti rotor; Beckman) for 16 h. A brown layer, which is the fraction containing IMVs, was recovered and precipitated by ultracentrifugation at 100,000 $\times g$ for 1 h. The pellet was suspended into 900 μl of solution A or B, divided into 300- μl aliquots, frozen by liquid nitrogen, and stored at -80°C until use.

Protein purification. Cells expressing FlgD, FlgE, or the FliH₂/FliI complex were suspended in solution C (50 mM Tris-HCl, pH 8.0, 500 mM NaCl) and disrupted by sonication. After removal of the cell debris by centrifugation, the supernatant was loaded onto a HisTrap HP (GE Healthcare) or nickel-nitrilotriacetic acid (Ni-NTA) agarose column (Qiagen), and proteins were eluted with imidazole solution. To remove the His tag, FlgD and FlgE solutions were incubated with thrombin (GE Healthcare) at room temperature for 3 h and then passed through the HiTrap benzamide FF column (GE Healthcare) to remove thrombin. The FliH₂/FliI complex was not treated with thrombin; therefore, the His tag of the complex was retained. Finally, proteins were purified using a Superdex 200 column (GE Healthcare) equilibrated with solution B. Cells expressing FliK were suspended in solution D (50 mM Tris-HCl, pH 8.0, 150 mM NaCl) and disrupted by sonication. After removal of the cell debris by centrifugation, supernatant was loaded onto a HisTrap HP (GE Healthcare) column, and proteins were eluted with imidazole solution. To remove the His tag, FliK solution was incubated with thrombin (GE Healthcare) at room temperature for 2 h and then dialyzed with solution A. The FliK solution was passed through the HisTrap HP (GE Healthcare) column to remove His-tag-retaining FliK and then passed through a HiTrap benzamide FF column (GE Healthcare) to remove thrombin. Finally, proteins were purified using a Superdex 200 column (GE Healthcare) equilibrated with solution B. FliI and FliJ were purified as previously reported in the crystallographic reports (8, 9). Each protein and protein complex eluted as a symmetrical peak corresponding to the expected molecular weight for the products. The purity of the purified proteins was examined by SDS-PAGE.

Transport assay. Three hundred microliters of the frozen stock solution of IMVs was thawed at room temperature and homogenized 10 times through an 0.8- μm polycarbonate membrane with the Avanti Mini-Extruder (Avanti Polar Lipids). The IMV solution was loaded on the Sephadex G50 fine column (GE Healthcare) equilibrated with solution B, and the IMV solution was eluted with 1.5 ml of solution B. The transport assay solution was prepared by mixing 100 μl of the IMV solution with 375 μl of external buffer containing Tris-HCl, pH 7.5, KCl, MgCl₂, dithiothreitol (DTT), and purified substrate proteins, and protein export was initiated by adding 25 μl of 0.1 M ATP solution. The ATP solution was prepared by dissolving ATP (dipotassium salt) in Tris-HCl solution (final concentration of 20 mM) followed by neutralization with KOH. The final reaction mixture contained 20 mM Tris-HCl, pH 7.5, 115 mM or 133 mM KCl, 5 mM MgCl₂, 1 mM DTT, and 5 mM ATP. The concentration of each chemical component in the external buffer was adjusted to match these values. After incubation at 37°C for 1 h, proteinase K was added at a final concentration of 10 $\mu\text{g/ml}$ to stop the transport reaction, and the reaction mixture was further incubated for 30 min to degrade nontransported substrate molecules. The assay mixture was ultracentrifuged at 100,000 $\times g$ for 30 min, and the precipitant containing IMV was washed by 1 ml of solution B. After removal of the washing buffer, the precipitant was incubated with 1 ml of solution B containing 10 $\mu\text{g/ml}$ proteinase K for 10 min at room temperature, followed by washing again with 1 ml of solution B, and then IMVs were dissolved with 45 μl of 1% (vol/vol) Triton X-100. The transported proteins were precipitated by trichloroacetate and were detected by immunoblotting analyses with polyclonal anti-FlgD or anti-FlgE antibody.

Purification of the hook-basal body from IMV. The hook-basal body complexes were purified according to the method shown by Aizawa et al. with minor modification (49). After the transport reaction, a part of the IMV solution was treated with 0.1% (vol/vol) Triton X-100 and ultracentrifuged (150,000 $\times g$, 30 min). The precipitates containing the hook-basal body were suspended in TET solution

(10 mM Tris-HCl, pH 8.0, 1 mM EDTA, 0.1% [vol/vol] Triton X-100), and the alkali solution (10% [wt/vol] sucrose, 0.1% [vol/vol] Triton X-100, 0.1 M KCl; pH was adjusted to 11 by KOH) was added to the suspension to completely dissolve the membrane. The suspension was layered on an equal volume of the 35% (wt/vol) sucrose solution prepared by dissolving sucrose in the TET solution in an ultracentrifuge tube, incubated on ice for 30 min, and ultracentrifuged at 38,000 rpm (Beckman TLA100.3 rotor) for 30 min to precipitate the hook-basal body. The precipitates were suspended in the TET solution and then observed by electron microscopy.

Electron cryotomography. R0.6/1.0 Quantifoil grids (Quantifoil Micro Tools, Jena, Germany) were glow discharged and pretreated with a solution of 10-nm colloidal gold particles (MP Biomedicals, USA). A 2.6- μ l solution of purified IMV was applied to the grid. The grids were blotted briefly with filter paper and then were rapidly plunged into liquid ethane using Vitrobot Mark II (FEI) for freezing. Electron microscopy images were collected at the liquid nitrogen temperature using a Titan Krios electron microscope (FEI) equipped with a field emission gun and a Falcon II direct electron detector (FEI). The microscope was operated at 300 kV and a nominal magnification of $\times 37,000$ with a calibrated pixel size of 4.46 Å after 2×2 binning. Images of single-axis tilt series were collected covering an angular range from -70° to $+70^\circ$ with a nonlinear Saxton tilt scheme at 4- to 7- μ m underfocus using the Xplore three-dimensional (3D) software package (FEI) and a cumulative dose of $\sim 120 \text{ e}^-/\text{Å}^2$. The IMOD package (50) was used to align tilted projection images and to generate the final 3D density map from the aligned image stack. The final 3D density map was obtained by the simultaneous iterative reconstruction technique (SIRT).

Negative-staining electron microscopy. Sample solutions were applied to carbon-coated copper grids and negatively stained with 2.0% (wt/vol) phosphotungstic acid or 2.0% (wt/vol) uranyl acetate. The samples for the hook length measurement were stained at 4°C to make the hooks straight. Images were observed with a JEM-1011 transmission electron microscope (JEOL, Tokyo, Japan) operating at 100 kV using a TVIPS TemCam-F114 charge-coupled device (CCD) camera or a TemCam-F415 CCD camera.

SUPPLEMENTAL MATERIAL

Supplemental material for this article may be found at <https://doi.org/10.1128/mBio.00988-18>.

FIG S1, TIF file, 1.6 MB.

FIG S2, TIF file, 2.4 MB.

FIG S3, TIF file, 1.1 MB.

FIG S4, TIF file, 2 MB.

FIG S5, TIF file, 2.7 MB.

FIG S6, TIF file, 2.6 MB.

TABLE S1, DOCX file, 0.03 MB.

ACKNOWLEDGMENTS

We thank H. Mori at Kyoto University for invaluable discussions and S. Kobashi and M. Kinoshita for technical support for purification of proteins.

This work was supported in part by JSPS KAKENHI grant numbers 15H02386 (to K.I.), 21227006 and 25000013 (to K.N.), and 26293097 (to T.M.) and MEXT KAKENHI grant numbers 23115008 (to K.I.) and 15H01640 (to T.M.).

REFERENCES

- Macnab RM. 2004. Type III flagellar protein export and flagellar assembly. *Biochim Biophys Acta* 1694:207–217. <https://doi.org/10.1016/j.bbamcr.2004.04.005>.
- Minamino T, Imada K, Namba K. 2008. Mechanisms of type III protein export for bacterial flagellar assembly. *Mol Biosyst* 4:1105–1115. <https://doi.org/10.1039/b808065h>.
- Terashima H, Kawamoto A, Morimoto YV, Imada K, Minamino T. 2017. Structural differences in the bacterial flagellar motor among bacterial species. *Biophys Physicobiol* 14:191–198. <https://doi.org/10.2142/biophysico.14.0.191>.
- Fukumura T, Makino F, Dietsche T, Kinoshita M, Kato T, Wagner S, Namba K, Imada K, Minamino T. 2017. Assembly and stoichiometry of the core structure of the bacterial flagellar type III export gate complex. *PLoS Biol* 15:e2002281. <https://doi.org/10.1371/journal.pbio.2002281>.
- Cornelis GR. 2006. The type III secretion injectisome. *Nat Rev Microbiol* 4:811–825. <https://doi.org/10.1038/nrmicro1526>.
- Kawamoto A, Morimoto YV, Miyata T, Minamino T, Hughes KT, Kato T, Namba K. 2013. Common and distinct structural features of *Salmonella* injectisome and flagellar basal body. *Sci Rep* 3:3369. <https://doi.org/10.1038/srep03369>.
- Fan F, Macnab RM. 1996. Enzymatic characterization of FliI: an ATPase involved in flagellar assembly in *Salmonella typhimurium*. *J Biol Chem* 271:31981–31988. <https://doi.org/10.1074/jbc.271.50.31981>.
- Imada K, Minamino T, Tahara A, Namba K. 2007. Structural similarity between the flagellar type III ATPase FliI and F_1 -ATPase subunits. *Proc Natl Acad Sci U S A* 104:485–490. <https://doi.org/10.1073/pnas.0608090104>.
- Ibuki T, Imada K, Minamino T, Kato T, Miyata T, Namba K. 2011. Common architecture of the flagellar type III protein export apparatus and F- and V-type ATPases. *Nat Struct Mol Biol* 18:277–282. <https://doi.org/10.1038/nsmb.1977>.
- Imada K, Minamino T, Uchida Y, Kinoshita M, Namba K. 2016. Insight into the flagella type III export revealed by the complex structure of the type III ATPase and its regulator. *Proc Natl Acad Sci U S A* 113:3633–3638. <https://doi.org/10.1073/pnas.1524025113>.
- Minamino T, Macnab RM. 2000. FliH, a soluble component of the type III flagellar export apparatus of *Salmonella*, forms a complex with FliI and inhibits its ATPase activity. *Mol Microbiol* 37:1494–1503. <https://doi.org/10.1046/j.1365-2958.2000.02106.x>.
- González-Pedrajo B, Fraser GM, Minamino T, Macnab RM. 2002. Molecular dissection of *Salmonella* FliH, a regulator of the ATPase FliI and the

- type III flagellar protein export pathway. *Mol Microbiol* 45:967–982. <https://doi.org/10.1046/j.1365-2958.2002.03047.x>.
13. Minamino T, Yoshimura SDJ, Morimoto YV, González-Pedraza B, Kami-ike N, Namba K. 2009. Roles of the extreme N-terminal region of FliH for efficient localization of the FliH-FliI complex to the bacterial flagellar type III export apparatus. *Mol Microbiol* 74:1471–1483. <https://doi.org/10.1111/j.1365-2958.2009.06946.x>.
 14. Thomas J, Stafford GP, Hughes C. 2004. Docking of cytosolic chaperone-substrate complexes at the membrane ATPase during flagellar type III protein export. *Proc Natl Acad Sci U S A* 101:3945–3950. <https://doi.org/10.1073/pnas.0307223101>.
 15. Imada K, Minamino T, Kinoshita M, Furukawa Y, Namba K. 2010. Structural insight into the regulatory mechanisms of interactions of the flagellar type III chaperone FliT with its binding partners. *Proc Natl Acad Sci U S A* 107:8812–8817. <https://doi.org/10.1073/pnas.1001866107>.
 16. Minamino T, Kinoshita M, Imada K, Namba K. 2012. Interaction between FliI ATPase and a flagellar chaperone FliT during bacterial flagellar protein export. *Mol Microbiol* 83:168–178. <https://doi.org/10.1111/j.1365-2958.2011.07924.x>.
 17. Minamino T, Kinoshita M, Inoue Y, Morimoto YV, Ihara K, Koya S, Hara N, Nishioka N, Kojima S, Homma M, Namba K. 2016. FliH and FliI ensure efficient energy coupling of flagellar type III protein export in *Salmonella*. *Microbiologyopen* 5:424–435. <https://doi.org/10.1002/mbo3.340>.
 18. Minamino T, Namba K. 2008. Distinct roles of the FliI ATPase and proton motive force in bacterial flagellar protein export. *Nature* 451:485–488. <https://doi.org/10.1038/nature06449>.
 19. Paul K, Erhardt M, Hirano T, Blair DF, Hughes KT. 2008. Energy source of flagellar type III secretion. *Nature* 451:489–492. <https://doi.org/10.1038/nature06497>.
 20. Minamino T, Morimoto YV, Hara N, Aldridge PD, Namba K. 2016. The bacterial flagellar type III export gate complex is a dual fuel engine that can use both H⁺ and Na⁺ for flagellar protein export. *PLoS Pathog* 12:e1005495. <https://doi.org/10.1371/journal.ppat.1005495>.
 21. Minamino T, Morimoto YV, Hara N, Namba K. 2011. An energy transduction mechanism used in bacterial flagellar type III protein export. *Nat Commun* 2:475. <https://doi.org/10.1038/ncomms1488>.
 22. Minamino T, Morimoto YV, Kinoshita M, Aldridge PD, Namba K. 2014. The bacterial flagellar protein export apparatus processively transports flagellar proteins even with extremely infrequent ATP hydrolysis. *Sci Rep* 4:7579. <https://doi.org/10.1038/srep07579>.
 23. Akeda Y, Galán JE. 2005. Chaperone release and unfolding of substrates in type III secretion. *Nature* 437:911–915. <https://doi.org/10.1038/nature03992>.
 24. Erhardt M, Mertens ME, Fabiani FD, Hughes KT. 2014. ATPase-independent type-III protein secretion in *Salmonella enterica*. *PLoS Genet* 10:e1004800. <https://doi.org/10.1371/journal.pgen.1004800>.
 25. Müller M, Blobel G. 1984. *In vitro* translocation of bacterial proteins across the plasma membrane of *Escherichia coli*. *Proc Natl Acad Sci U S A* 81:7421–7425. <https://doi.org/10.1073/pnas.81.23.7421>.
 26. Yamane K, Ichihara S, Mizushima S. 1987. *In vitro* translocation of protein across *Escherichia coli* membrane vesicles requires both the proton motive force and ATP. *J Biol Chem* 262:2358–2362.
 27. Bageshwar UK, Musser SM. 2007. Two electrical potential-dependent steps are required for transport by the *Escherichia coli* Tat machinery. *J Cell Biol* 179:87–99. <https://doi.org/10.1083/jcb.200702082>.
 28. Aldridge C, Poonchareon K, Saini S, Ewen T, Solovyva A, Rao CV, Imada K, Minamino T, Aldridge PD. 2010. The interaction dynamics of a negative feedback loop regulates flagellar number in *Salmonella enterica* serovar Typhimurium. *Mol Microbiol* 78:1416–1430. <https://doi.org/10.1111/j.1365-2958.2010.07415.x>.
 29. Ohnishi K, Ohto Y, Aizawa S, Macnab RM, Iino T. 1994. FlgD is a scaffolding protein needed for flagellar hook assembly in *Salmonella typhimurium*. *J Bacteriol* 176:2272–2281. <https://doi.org/10.1128/jb.176.8.2272-2281.1994>.
 30. Homma M, Iino T. 1985. Locations of hook-associated proteins in flagellar structures of *Salmonella typhimurium*. *J Bacteriol* 162:183–189.
 31. Fraser GM, Hirano T, Ferris HU, Devgan LL, Kihara M, Macnab RM. 2003. Substrate specificity of type III flagellar protein export in *Salmonella* is controlled by subdomain interactions in FliH. *Mol Microbiol* 48:1043–1057. <https://doi.org/10.1046/j.1365-2958.2003.03487.x>.
 32. Abrusci P, Vergara-Irigaray M, Johnson S, Beeby MD, Hendrixson DR, Roversi P, Friede ME, Deane JE, Jensen GJ, Tang CM, Lea SM. 2013. Architecture of the major component of the type III secretion system export apparatus. *Nat Struct Mol Biol* 20:99–104. <https://doi.org/10.1038/nsmb.2452>.
 33. Chen S, Beeby M, Murphy GE, Leadbetter JR, Hendrixson DR, Briegel A, Li Z, Shi J, Tocheva EI, Müller A, Dobro MJ, Jensen GJ. 2011. Structural diversity of bacterial flagellar motors. *EMBO J* 30:2972–2981. <https://doi.org/10.1038/emboj.2011.186>.
 34. Bai F, Morimoto YV, Yoshimura SD, Hara N, Kami-ike N, Namba K, Minamino T. 2014. Assembly dynamics and the roles of FliI ATPase of the bacterial flagellar export apparatus. *Sci Rep* 4:6528. <https://doi.org/10.1038/srep06528>.
 35. Moriya N, Minamino T, Hughes KT, Macnab RM, Namba K. 2006. The type III flagellar export specificity switch is dependent on FliK ruler and a molecular clock. *J Mol Biol* 359:466–477. <https://doi.org/10.1016/j.jmb.2006.03.025>.
 36. Kazetani K, Minamino T, Miyata T, Kato T, Namba K. 2009. ATP-induced FliI hexamerization facilitates bacterial flagellar protein export. *Biochem Biophys Res Commun* 388:323–327. <https://doi.org/10.1016/j.bbrc.2009.08.004>.
 37. Fraser GM, Bennett JCQ, Hughes C. 1999. Substrate-specific binding of hook-associated proteins by FlgN and FliT, putative chaperones for flagellum assembly. *Mol Microbiol* 32:569–580. <https://doi.org/10.1046/j.1365-2958.1999.01372.x>.
 38. Auvray F, Thomas J, Fraser GM, Hughes C. 2001. Flagellin polymerisation control by a cytosolic export chaperone. *J Mol Biol* 308:221–229. <https://doi.org/10.1006/jmbi.2001.4597>.
 39. Bennett JC, Thomas J, Fraser GM, Hughes C. 2001. Substrate complexes and domain organization of the *Salmonella* flagellar export chaperones FlgN and FliT. *Mol Microbiol* 39:781–791. <https://doi.org/10.1046/j.1365-2958.2001.02268.x>.
 40. Aldridge P, Karlinsey JE, Hughes KT. 2003. The type III secretion chaperone FlgN regulates flagellar assembly via a negative feedback loop containing its chaperone substrates FlgK and FlgL. *Mol Microbiol* 49:1333–1345. <https://doi.org/10.1046/j.1365-2958.2003.03637.x>.
 41. Bange G, Kümmerer N, Engel C, Bozkurt G, Wild K, Sinning I. 2010. FliH provides the adaptor for coordinated delivery of late flagella building blocks to the type III secretion system. *Proc Natl Acad Sci U S A* 107:11295–11300. <https://doi.org/10.1073/pnas.1001383107>.
 42. Kinoshita M, Hara N, Imada K, Namba K, Minamino T. 2013. Interactions of bacterial flagellar chaperone-substrate complexes with FliH contribute to co-ordinating assembly of the flagellar filament. *Mol Microbiol* 90:1249–1261. <https://doi.org/10.1111/mmi.12430>.
 43. Evans LD, Poulter S, Terentjev EM, Hughes C, Fraser GM. 2013. A chain mechanism for flagellum growth. *Nature* 504:287–290. <https://doi.org/10.1038/nature12682>.
 44. Inoue Y, Morimoto YV, Namba K, Minamino T. 2018. Novel insights into the mechanism of well-ordered assembly of bacterial flagellar proteins in *Salmonella*. *Sci Rep* 8:1787. <https://doi.org/10.1038/s41598-018-20209-3>.
 45. Hirano T, Minamino T, Namba K, Macnab RM. 2003. Substrate specificity classes and the recognition signal for *Salmonella* type III flagellar export. *J Bacteriol* 185:2485–2492. <https://doi.org/10.1128/JB.185.8.2485-2492.2003>.
 46. Dreyfus G, Williams AW, Kawagishi I, Macnab RM. 1993. Genetic and biochemical analysis of *Salmonella typhimurium* FliI, a flagellar protein related to the catalytic subunit of the F₁F₀ ATPase and to virulence proteins of mammalian and plant pathogens. *J Bacteriol* 175:3131–3138. <https://doi.org/10.1128/jb.175.10.3131-3138.1993>.
 47. Fujii T, Kato T, Hiraoka KD, Miyata T, Minamino T, Chevance FFV, Hughes KT, Namba K. 2017. Identical folds used for distinct mechanical functions of the bacterial flagellar rod and hook. *Nat Commun* 8:14276. <https://doi.org/10.1038/ncomms14276>.
 48. Morimoto YV, Kamiike N, Miyata T, Kawamoto A, Kato T, Namba K, Minamino T. 2016. High-resolution pH imaging of living bacterial cells to detect local pH differences. *mBio* 7:e01911-16. <https://doi.org/10.1128/mBio.01911-16>.
 49. Aizawa SI, Dean GE, Jones CJ, Macnab RM, Yamaguchi S. 1985. Purification and characterization of the flagellar hook-basal body complex of *Salmonella typhimurium*. *J Bacteriol* 161:836–849.
 50. Kremer JR, Mastrorade DN, McIntosh JR. 1996. Computer visualization of three-dimensional image data using IMOD. *J Struct Biol* 116:71–76. <https://doi.org/10.1006/jsbi.1996.0013>.